

Quantum transport modeling of Fe/MgO/Fe magnetic tunnel junction with FeO_{0.5} buffer layer: the effects of correlations

V. Timoshevskii,* Yibin Hu, É. Marcotte, and Hong Guo

Department of Physics, McGill University, 3600 rue University, Montréal, Québec, Canada H3A 2T8
(Dated: July 18, 2018)

We report *ab initio* simulations of quantum transport properties of Fe/MgO/Fe trilayer structures with FeO_{0.5} buffer iron oxide layer, where on-site Coulomb interaction is explicitly taken into account by local density approximation + Hubbard U approach. We show that on-site Coulomb repulsion in the iron-oxygen layer can cause a dramatic drop of the tunnel magnetoresistance of the system. We present an understanding of microscopic details of this phenomenon, connecting it to localization of the Fermi electrons of particular symmetry, which takes place in the buffer Fe-O layer, when on-site Coulomb repulsion is introduced. We further study the possible influence of the symmetry reduction in the buffer Fe-O layer on the transport properties of the Fe/MgO/Fe interface.

PACS numbers: 85.35.-p, 72.25.-b, 85.65.+h, 73.20.-r

I. INTRODUCTION

Due to its high tunnel magnetoresistance (*TMR*), studying of Fe/MgO/Fe magnetic tunnel junctions (MTJ) has evolved into an active research area during last decade. Indeed, the *TMR* value of 180-250%, reported by several research groups for MgO-based systems^{1,2}, is the highest *TMR*, experimentally measured at room temperature. These high values of tunnel magnetoresistance make the MgO-based MTJs excellent candidates for spintronics applications: magnetic random access memory³, programmable logic elements⁴, and magnetic read sensors.

Since the original theoretical prediction⁵ of large *TMR* effect in Fe/MgO/Fe interfaces, atomic-level simulations played a key role in understanding of unusually high *TMR* values in these systems, and a lot of progress has been achieved in this field. Butler *et al*⁵, using a Korringa-Kohn-Rostoker (KKR) technique, has provided an elegant explanation of physics behind the Fe/MgO/Fe magnetoresistance, connecting it with the match of the symmetry of the Bloch states in the electrodes with the symmetry of the evanescent states of the MgO barrier. Later, Waldron *et al*⁶, employing Non-Equilibrium Green's Function (NEGF) formalism, combined with Density Functional Theory (DFT), explained a voltage

dependence of *TMR* in Fe/MgO/Fe interfaces. However, there is still an important issue which is the *quantitative* understanding of physics behind Fe/MgO/Fe system: the absolute values of experimentally observed *TMR* ratios cannot be reproduced by *ab initio* simulations if assuming ideal device models: these ideal models predicts much larger *TMR* than that has been observed. There may be a number of reasons behind the theory/experimental discrepancy such as oxygen vacancies in the MgO layer^{7,8}, the existence of a FeO buffer monolayer^{9,10}, other atomic defects¹¹, and interface roughness⁶. These structural imperfections are clearly detrimental but may be overcome by improving the material quality and the fabrication process of the devices. It is the purpose of this work to investigate a possible *physical* reason - as opposed to the *structural* reason, for the reduced *TMR* value as observed experimentally.

In particular, we theoretically investigate an important piece of physics that is related to the presence of a FeO buffer monolayer formed as a result of electrode oxygenation during the MgO deposition⁹. Calculations already demonstrated¹⁰ a reduction of *TMR* from that of the ideal device structure in the presence of the FeO layer, although even at 60% oxygen concentration in the layer, the predicted *TMR* is still much greater than that observed experimentally. On the other hand, it is well known that *bulk* FeO crystal is a Mott-Hubbard insulator whose electronic structure cannot be correctly predicted by Local Spin Density Approximation (LSDA) commonly used in density functional theory (DFT) calculations. This is due to an incorrect treatment of strong correlation in the FeO compound, as such LSDA predicts FeO to be metallic while in reality it is an insulator with a well-developed band gap. It is therefore very interesting to ask if a strong correlation exists in the single monolayer of FeO_{1-x} that is at the interface of between Fe and MgO in the Fe/MgO/Fe trilayer so as to influence *TMR*. If it does, a localization of the Fe 3*d*-states is expected that may lead to a substantial drop of transmission coefficients for both up- and down-spin channels and, as a result, to a significant change of *TMR*. To our

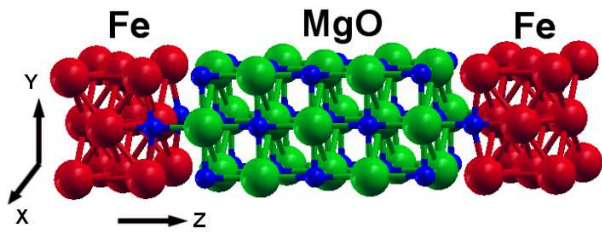


FIG. 1: Atomic structure of the two-probe Fe/MgO/Fe device with FeO_{0.5}O buffer layer. The system is periodic in the directions (X, Y) parallel to the interface. The leads are semi-infinite in Z -direction.

knowledge, the only attempt to take into account correlation effects in FeO layer in Fe/MgO/Fe interface was taken by Mirhosseini *et al*¹², who applied self-interaction correction (SIC) to LSDA to calculate spin conductance and magnetoresistance of Fe/FeO/MgO/FeO/Fe. These authors obtained a significant increase of the binding energies of Fe 3*d*-states in the “spin-up” channel in FeO layer. As a result, it was found that SIC-corrected treatment moderately reduces the TMR ratio at energies below the Fermi level (E_F), from where the Fe 3*d* majority states are removed, while a 10% increase of TMR at E_F and above is observed. Since correlation effects may be important and it is a very complicated problem, further investigation along this line is warranted.

Here we present results of our first principles calculations of quantum transport properties in Fe/MgO/Fe interface with FeO_{0.5} iron-oxide separation layer with the oxygen content close to the experimental one (60%). We use a state-of-the-art quantum transport technique based on density functional theory (DFT) combined with Keldysh nonequilibrium Green’s function (NEGF) formalism¹³. The correlation effects in FeO_{0.5} layer are taken into account within the LDA+ U approach which explicitly adds the on-site Coulomb repulsion energy (U) for Fe 3*d*-states directly to the DFT Hamiltonian. The value of U is calculated from first principles for a particular atomic structure of the interface using a constrained LDA technique¹⁴. Our results demonstrate that the consideration of correlation effects in the FeO_{1-x} layer leads to a dramatic drop of magnetoresistance in Fe/MgO/Fe interface, and brings it to the values comparable to that observed in experiments. The microscopic details of this substantial TMR reduction can be understood by analyzing the effects of electron localization on scattering states of different symmetry.

II. CALCULATION DETAILS

A. Interface structure

We consider a model Fe/MgO/Fe interface structure with five layers of magnesium oxide stacked between two semi-infinite Fe-bcc electrodes, oriented in the (100) direction (Fig. 1). The system is periodic in the plane transverse to the interface direction. The unit cell vectors in this plane are rotated 45° with respect to Fe-bcc unit cell, and their lengths equal $a\sqrt{2}$, where a is the cell parameter of Fe-bcc lattice. This choice of the system geometry allowed us to model the interface FeO monolayer on each side of MgO slab with 50% oxygen occupation (Fig. 1), which is close to 60%, observed experimentally by Meyerheim *et al*⁹. The structure geometry was completely relaxed with respect to atomic positions and interlayer distances using highly accurate all-electron Linearized Augmented Plane Wave Method (LAPW) as implemented in Wien2k¹⁵ program package. We paid special attention to geometrical properties of the inter-

face, as the earlier study of Waldron *et al* demonstrated a substantial change in TMR, when the interface atoms are displaced by only 1% of their bond length⁶. Our theoretical optimized geometry showed a good agreement with results of X-ray diffraction experiments performed for the MTJs having 60% oxygen content of the interface FeO layer⁹. In particular, the obtained Fe-O distances within the interface FeO layer and between FeO and MgO layers were found to be 2.03Å and 2.38Å respectively, which are in very good agreement with experimental data (2.03Å and 2.35Å).

Having obtained the relaxed geometry of the interface, we proceed to calculate the electronic transport properties. We used the MatDcal program package¹⁶ which is a DFT-based code, employing a state-of-the-art quantum transport technique based on the Keldysh nonequilibrium Green’s function (NEGF) formalism. The method uses standard norm-conserving pseudopotentials¹⁷ and an s , p , d double-zeta LCAO-type basis set. The NEGF-DFT formalism is excellently suited for self-consistent electronic transport calculations of multi-atom interfaces with non-periodic (open) boundary conditions. A detailed description of theoretical base of the method can be found in our previous publications^{13,18}. We found a 20×20 K -point mesh to be sufficient for self-consistent calculations of the two-probe device. Much denser ($10^3 \times 10^3$) sampling was further used for calculation of transmission coefficient T . A TMR ratio was calculated at zero bias voltage using the following formula: $TMR = (T_{\uparrow\uparrow} - T_{\uparrow\downarrow})/T_{\uparrow\downarrow}$, where $T_{\uparrow\uparrow}$ and $T_{\uparrow\downarrow}$ correspond to transmission coefficients calculated at the Fermi energy for parallel and anti-parallel spin configurations of iron leads.

B. Correlation effects

To study the effects of electron localization on electronic transport, we went beyond the standard NEGF-DFT formalism, and implemented the LDA+ U scheme into the MatDcal code. We followed the original works of Anisimov *et al*^{14,19,20}, and details of our implementation of the LDA+ U method within NEGF formalism is summarized in the Appendix. According to the philosophy of LDA+ U approach, the atomic system is divided into the weakly-correlated part where the exchange-correlation is treated within LDA; and a strongly-correlated part where the Coulomb (U) and exchange (J) energies of interaction of two electrons on the same atom are explicitly taken into account. In the case of oxidated Fe/MgO/Fe system, we treat the interface FeO_{0.5} layer where we expect the electron localization to play a major role as a highly correlated subsystem and apply LDA + U treatment to the Fe-3*d* states of this layer.

To correctly apply the LDA + U method, proper values of U and J parameters need to be supplied. These parameters are usually either taken from experimental data, or a series of calculations are performed for dif-

ferent values of U and J to check how the results depend on them. In our case, we have a single monolayer of $\text{FeO}_{0.5}$ sandwiched between an Fe electrode and the MgO barrier. To our knowledge, no experimental data about the on-site Coulomb repulsion energy in this type of interfaces have been reported, hence we have calculated it from first principles. Note that the U parameter, defined as the cost in Coulomb energy to place two electrons at the same site¹⁴, can be calculated by following the original ideas of Anisimov and Gunnarsson¹⁴ within their particular implementation of the LAPW method, proposed by Madsen and Novák²¹. In our calculations, a supercell parallel to the interface plane was constructed, and the hybridization of $3d$ -states of one of the Fe atoms in the $\text{FeO}_{0.5}$ layer with all other orbitals was switched off. By performing a series of self-consistent calculations for this system with different values of occupation numbers of this artificially atomized $3d$ -shell, we calculated the $U_{eff} = U - J$ parameter as a difference between the corresponding eigenvalues²¹. This way, we found that the effective Coulomb repulsion for Fe $3d$ -electrons in the interface $\text{FeO}_{0.5}$ layer is about 4.6 eV . This value is somewhat smaller than the one calculated by Anisimov *et al* for bulk FeO crystal (5.9 eV)¹⁹. The reduction of U in our system is expected due to the presence of the Fe electrode on one side of the $\text{FeO}_{0.5}$ layer: the free electrons in the Fe electrode increase the screening of the on-site Coulomb repulsion in the $\text{FeO}_{0.5}$.

III. RESULTS AND DISCUSSION

A. TMR ratio

First, we performed full self-consistent calculations of the interface for Parallel (PC) and Anti-Parallel (APC) spin configurations of Fe leads for the cases of $U_{eff} = 0$, as well as with “turned on” Coulomb repulsion. Further, for the case of each U -value, a contribution to transmission coefficient from spin-up and spin-down channels has been obtained, as well as a final value of TMR -ratio. The obtained results are summarized in Table I. The most striking result is the dramatic drop of the TMR value for as soon as on-site Coulomb repulsion is taken into account for Fe $3d$ -electrons in the $\text{FeO}_{0.5}$ interface layer.

For a pure LSDA calculation ($U_{eff} = 0$), we obtain a TMR of 1942%, which is of the same order

TABLE I: Calculated contributions to transmission coefficient ($\times 10^{-6}$) from different spin channels for the cases of $U = 0$ and $U = 4.6 \text{ eV}$. The calculated TMR ratio is also provided.

Configuration	T_{\uparrow}	T_{\downarrow}	TMR	U_{eff}
PC	95.57	0.81	1942%	0.0 eV
APC	2.56	2.16		
PC	2.08	0.47	60%	4.6 eV
APC	0.80	0.80		

of magnitude as the results obtained in other similar calculations⁶, as well as the LDA results obtained for oxygenated Fe/MgO/Fe interfaces ($\sim 1500\%$)¹⁰. As soon as Coulomb repulsion of 4.6 eV is taken into account, the TMR ratio drops dramatically down to 60%. To trace the origin of this drop, we analyze the transmission contributions to TMR from different spin channels for PC and APC (Table I). We notice that the transmission in APC for both spin channels reduces by a factor of ~ 3 when Coulomb repulsion is introduced. Even smaller is a reduction in spin-down channel for both PC and APC (factor of $\sim 1.7 - 2.7$). A really defining drop in transmission is observed in the spin-up channel for the case of PC. In this case the transmission coefficient drops by a factor of 46, which constitutes a principal reason behind the dramatic reduction of TMR .

We should note that our LDA+ U results are somewhat opposite to those of Mirhosseini *et al*¹², who used the SIC-corrected LDA approach. We clearly see a significant drop of TMR ratio upon “turning on” correlations in $\text{FeO}_{0.5}$ layer, while Mirhosseini *et al* did not observe significant changes of this quantity at energies equal or above the Fermi level. Further, our results demonstrate a principle reason of this drop - a dramatic reduction of transmission in the “spin-up” channel for PC, while the SIC correction mostly reduces the APC current.

B. Scattering states

To establish a more detailed physical picture, it is interesting to follow how the absolute square of the tunneling electron wavefunction (scattering state) changes along the tunneling direction. As the drop in TMR ratio is caused by substantial reduction of transmission in spin-up channel for PC, we calculate the scattering state for this particular spin channel in PC. Only states at the Γ -point and at the Fermi energy are considered.

In their pioneering theoretical study, Butler *et al*⁵ demonstrated that tunneling in the spin-up channel almost exclusively takes place through the state of Δ_1 symmetry, while other bands, crossing the Fermi level of the Fe lead, rapidly decay in the MgO barrier. In our system we also observe two low-decay scattering states with similar profile, while others decay faster in the MgO barrier. The presence of two of these states, as compared to Butler’s setup where there is only one state of Δ_1 symmetry, is explained by the choice of our unit cell, where there are two Fe atoms per layer in the direction perpendicular to tunneling. We plot the low-decay scattering states in Fig. 2. It can be noticed that these two states are substantially different. Even without the Coulomb repulsion U , there is a factor of 10^3 difference in the squared amplitude of these states after tunneling through the barrier.

To get insight into the physical origin of this difference, we calculate the spectral composition of the two scattering states, shown in figure 2, by projecting them on atomic orbitals of the interface Fe atoms. We were

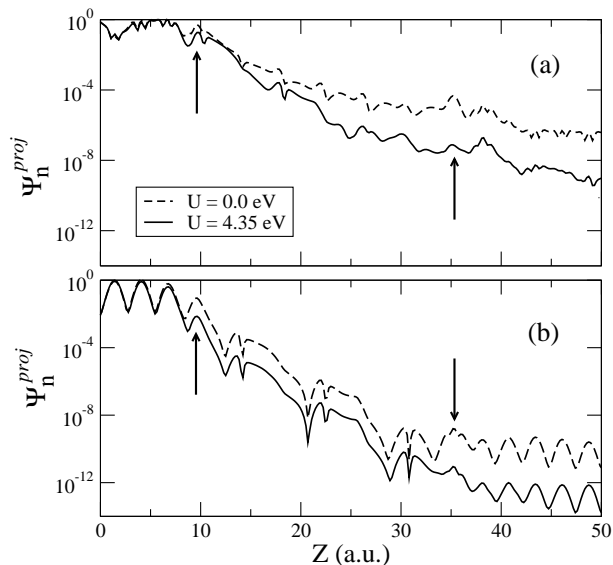


FIG. 2: Distribution of squared electronic wavefunction (scattering state) across the interface for two low-decay tunneling states of Fe/MgO/Fe interface with FeO_{0.5} buffer layer. The wavefunction is integrated in XY plane. Calculations are done at the Fermi energy, for spin-up channel and at the Γ -point only. The arrows mark the positions of the FeO_{0.5} layer on both sides of the interface.

surprised to find that the orbitals, forming the Δ_1 -state (s, d_{z^2}) in the system without FeO layer (or with 100%-populated FeO layer), were not the only ones forming these low-decay states in the case of our structure with FeO_{0.5} iron oxide layer. Additionally, a significant contribution of $d_{x^2-y^2}$ Fe states was found in both scattering states, presented in Fig.2. In fact, this contribution is comparable in value to the one of d_{z^2} orbital, and even exceeds it for one of the scattering states. The calculations with $U = 0$ showed that the contribution of d_{z^2} and $d_{x^2+y^2}$ orbitals is respectively equal to 54% and 30% for scattering state (a), and 19% and 56% for scattering state (b), Fig.2. We see that the scattering state (a) is mainly formed by the d_{z^2} states, while the $d_{x^2+y^2}$ orbitals mostly contribute to the formation of scattering state (b). This difference in electronic structure is the underlying reason of the significantly different decay rate of these two scattering states. A much lower tunneling amplitude of state (b) can be understood as follows. The $d_{x^2+y^2}$ orbitals, which contribute mostly to this state, are oriented in the XY plane (parallel to the interface), which reduces their overlap with p_z -orbitals of MgO layer. At the same time, the d_{z^2} orbitals, which dominate in the formation of scattering state (a), are oriented along the Z axis (perpendicular to the interface). This orientation increases their overlap with MgO oxygen states and therefore creates conditions for higher tunneling current.

C. Electron localization

Let us now concentrate on the scattering state Fig.2(a) which has the lowest decay rate, and therefore mostly contributes to the tunneling process. We see that “turning on” Coulomb repulsion U gives rise to a factor of ~ 300 drop in the squared amplitude of this state after tunneling through the barrier. To trace the physical origin of this substantial drop of transmission caused by the correlation effects in the FeO_{0.5} interface layer, we study the density of electronic states (DOS) of the system. As more than a half of this scattering state (54%) is contributed by Fe d_{z^2} orbitals, we concentrate on the behavior of Fe d_{z^2} states near the Fermi energy. Figure 3 shows the calculated DOS of d_{z^2} states of Fe atoms in the FeO_{0.5} interface layer. For the sake of comparison we plot the calculated DOS curves for $U = 4.6$ eV and $U = 0.0$ eV (standard LSDA). We see a substantial difference in behavior of Fe d_{z^2} -electrons for “up” and “down” channels upon “turning on” the Coulomb repulsion. For the spin-down states, the DOS at the Fermi level is practically unchanged, while for spin-up states it drops almost to zero when $U = 4.6$ eV is introduced. This is a well-known effect of LDA+ U : for the systems where correlation effects are strongly underestimated by standard LDA, the LDA+ U tends to split the DOS at the Fermi level into fully occupied and fully unoccupied peaks, significantly depleting DOS (or even forming the gap) at the Fermi level¹⁹.

The performed DOS analysis explains well the transmission data, summarized in Table I. Taking into account the correlation effects in the FeO_{0.5} layer gives rise to a dramatic reduction of the electronic density of states at the Fermi level in the spin-up channel, which effectively “turns off” these electrons from the transmission process. In Table I this is reflected as a large drop in transmission in the spin-up channel when a non-zero U is used in calculations. We decided to visualize this “turn-off” process for the d_{z^2} Fe electrons in the FeO_{0.5} layer by cal-

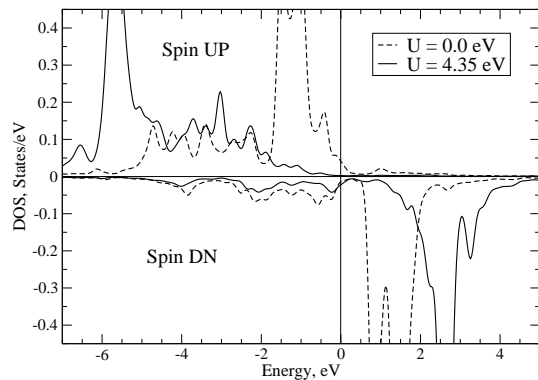


FIG. 3: Density of electronic states for the Fe electrons of d_{z^2} symmetry, calculated for the interface FeO_{0.5} layer. Both results for calculations with $U = 0.0$ eV and with $U = 4.35$ eV are presented.

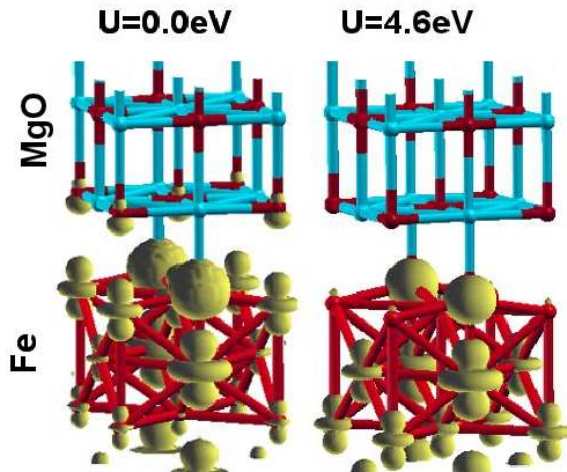


FIG. 4: Real-space distribution of electronic density at the Fermi energy, calculated with $U = 0.0 \text{ eV}$ (left panel), and with $U = 4.35 \text{ eV}$ (right panel) for oxidated Fe-MgO-Fe system. Only states, having d_{z^2} symmetry, are taken into account for Fe layers when calculating the density.

culating their real-space distribution, and checking how this distribution is changed when the Coulomb repulsion is considered. In Figure 4 we plot the calculated real-space density of spin-up Fermi electrons for the interface part of the Fe/MgO/Fe system. We show only the electrons with d_{z^2} -symmetry of the wavefunction for all Fe atoms, while states with all symmetries are taken into account for O and Mg atoms. This symmetry-based plotting allows us to trace the behavior only of those electrons which participate in the tunneling process. The picture shows that in the case of standard LSDA calculations (left panel), the interface $\text{FeO}_{0.5}$ layer carries a significant density of d_{z^2} Fermi electrons, and it is even comparable to the electronic density in the deeper layers of the Fe electrode. Moreover, these electrons couple with the oxygen p -electrons of the first MgO layer, creating a non-zero density of Fermi electrons on this layer. When the on-site Coulomb repulsion is turned on, the d_{z^2} electrons with the Fermi energies are almost absent in the $\text{FeO}_{0.5}$ layer, as well as in the first layer of the MgO barrier. This picture illustrates that the proper consideration of the correlation effects in the interface $\text{FeO}_{0.5}$ layer leads to the localization of the Fe electrons with d_{z^2} symmetry, which does not allow them to participate in the tunneling process and, as a result, is reflected as a dramatic reduction of the TMR characteristics of Fe/MgO/Fe system.

D. Low-decay states and the symmetry of $\text{FeO}_{0.5}$ layer

Let us now go back to the question of spectral composition of the two low-decay scattering states, shown in Fig.2. As we mentioned above, our calculations for the

system with $\text{FeO}_{0.5}$ interface layer showed the presence of Fe $d_{x^2-y^2}$ orbitals in the low-decay scattering states: they contribute 30% to the first lowest-decay state (Fig.2a) and are mostly forming (56%) the second one (Fig.2b). The orbitals of this symmetry do not contribute to the Δ_1 -state in case of non-oxidated Fe/MgO/Fe interface⁵, and in the following we shall try to understand the physical mechanisms of the influence of $\text{FeO}_{0.5}$ interface layer on the formation of the low-decay scattering states in Fe/MgO/Fe system.

Butler *et al*⁵ brought on the idea of “symmetry filtering” which appeared to be the central point of the elegant physical explanation of TMR effect in Fe/MgO/Fe trilayers. The authors demonstrated that Fe-bcc Bloch states of different symmetry show significantly different decay rates in the MgO barrier. The one with the smallest decay, which is able to couple to its counterpart in the opposite Fe lead, is that of Δ_1 symmetry. This state transforms as a linear combination of s , p_z , and d_{z^2} orbitals. The analysis of Butler *et al* is based on a perfect cubic symmetry of Fe-bcc, matching also perfect cubic unit cell of MgO (although rotated by 45°). In the case of 100%-oxidated buffer layer (FeO) the situation does not change, as the point symmetry of all Fe sites is the same as in non-oxidated interface. However, the situation may change significantly if a low-symmetry FeO_{1-x} layer is formed at the Fe/MgO/Fe interface. In this case the admixing of other electronic states to Δ_1 band may take place (strictly speaking, this low-decay band can not be classified as Δ_1 anymore.). This picture correlates well with our results for the interface with $\text{FeO}_{0.5}$ iron oxide layer. Although the distribution of oxygen in this layer is still ordered, the symmetry of Fe sites is changed. Therefore our structure can be a good model to test the effects of symmetry changes in FeO_{1-x} layer on the composition of the low-decay scattering state.

To clarify the role of symmetry of $\text{FeO}_{0.5}$ iron oxide layer in formation of the low-decay states in Fe/MgO/Fe interface, we now take a different approach and perform a group theory analysis of the interaction of Fe lead states with the FeO_{1-x} layer. In case of 100%-populated FeO layer, all interface Fe atoms are occupying the positions with C_{4v} point symmetry group. In this group the d -orbitals of iron and p -orbitals of oxygen of the first MgO layer transform according to the following irreducible representations: $A_1 \Rightarrow \{d_{z^2}, p_z\}$; $E \Rightarrow \{(d_{xz}, d_{yz}), p_x, p_y\}$; $B_1 \Rightarrow \{d_{xy}\}$; $B_2 \Rightarrow \{d_{x^2-y^2}\}$. In this case the A_1 orbitals are forming the Δ_1 band. This band is the only one having the admixture of O p_z -states, and has the lowest decay across the MgO barrier. The orbitals belonging to the two-dimensional representation E , form the Δ_5 band. This band is doubly-degenerate and has a significantly higher decay in the MgO barrier. Finally, the orbitals belonging to B_1 and B_2 representations form Δ_2' and Δ_2 bands, which are forbidden to interact with oxygen p -orbitals and show the highest decay in the MgO barrier. The results of this symmetry-based analysis are in excellent agreement with original physical

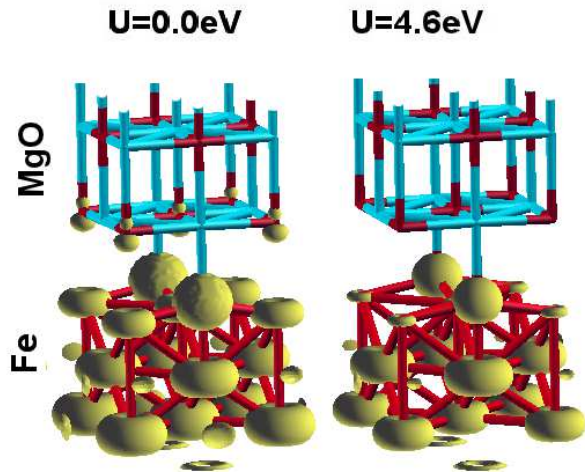


FIG. 5: The same quantity as in Fig.4, but calculated with contribution from Fe $d_{x^2-y^2}$ states only.

picture presented by Butler *et al*⁵.

Let us now perform the same analysis for the case of our $\text{FeO}_{0.5}$ interface layer, where the point symmetry of Fe atoms is reduced. In this system the interface iron atoms have C_{2v} point symmetry, and the interacting Fe d - and O p -orbitals belong to the following irreducible representations²²: $A_1 \Rightarrow \{d_{z^2}, p_z, d_{xy}\}$; $B_1 \Rightarrow \{(d_{xz} + d_{yz}), p_x\}$; $B_2 \Rightarrow \{(d_{xz} - d_{yz}), p_y\}$; $A_2 \Rightarrow \{d_{x^2-y^2}\}$. We immediately see the striking difference: the A_1 representation now includes both d_{z^2} and d_{xy} orbitals while in the case of fully-symmetric FeO layer, the d_{xy} orbitals were not allowed to interact with MgO p_z -states by symmetry rules. It is important to note here that due to the 45° rotation of the Fe electrode's unit cell in our calculation (as compared to the Fe-bcc unit cell), the calculated $d_{x^2-y^2}$ orbitals found to contribute significantly to the low-decay scattering states, are in fact the d_{xy} orbitals in Fe-bcc unit cell²². We see that our results of theoretical symmetry-based analysis excellently agree with the results of our numerical simulations. If we now speak the language of the symmetry bands, coming out of Fe-bcc (100) surface, we observe that introducing of ordered $\text{FeO}_{0.5}$ interface layer in Fe/MgO/Fe interface leads to the mixing of Δ_1 and $\Delta_{2'}$ bands and their interaction with p_z -states of oxygen in MgO layer. In this way, both Δ_1 and $\Delta_{2'}$ bands contribute now to the formation of low-decay scattering state in MgO barrier, which change significantly the TMR properties of the system.

To complete our study, it is interesting to check if “turning on” the Coulomb repulsion influences interface Fe $d_{x^2-y^2}$ states in the same way as it collapses the d_{z^2} -states studied above. We calculated the real-space distribution of electrons with the Fermi energy for both cases of $U = 0$ and $U = 4.35\text{eV}$, where only the contribution from $d_{x^2-y^2}$ orbitals is taken into account. The results are presented in Fig.5. We see that a non-zero Coulomb repulsion gives rise to a significant collapse of

the $d_{x^2-y^2}$ states in the $\text{FeO}_{0.5}$ layer. As a consequence, their coupling with oxygen states is dramatically reduced (notice the absence of charge in the first MgO layer for $U = 4.35\text{eV}$ case, Fig.5, right panel), which leads to the $d_{x^2-y^2}$ -states being practically “switched off” from the tunneling process. It is important to notice that the same effect should also take place in non-oxidated system, or in the system with 100%-oxidated FeO layer, but in those cases the $d_{x^2-y^2}$ states are forbidden to interact with oxygen by symmetry and therefore this collapse should not influence in any way the tunneling characteristics of the interface.

IV. CONCLUSION

In conclusion, we presented the results of *ab initio* calculations of transport properties of Fe/MgO/Fe interface with $\text{FeO}_{0.5}$ buffer layer. By combining NEGF-DFT formalism with the LDA+ U approach, we explicitly took into account the on-site Coulomb repulsion in the Fe-O interface layer, where the U -value was calculated from the first principles for a particular interface structure. Our results demonstrate a dramatic drop of TMR characteristic of the interface (down to $\sim 60\%$), when Coulomb repulsion is taken into account in the $\text{FeO}_{0.5}$ buffer layer. This reduction is found to be mostly due to a dramatic drop of transmission in spin-up channel for parallel configuration of iron leads. By analyzing the distribution of scattering states across the interface, as well as a real-space distribution of the Fermi electrons with a particular symmetry of the wavefunction, we traced the physical origin of this transmission reduction. The results showed that for 50%-oxidated buffer layer ($\text{FeO}_{0.5}$), this TMR drop is caused by a spacial collapse of Fe d_{z^2} and $d_{x^2-y^2}$ electronic states at the Fermi level when non-zero U -value is taken into account. Finally, we used the methods of group theory and studied the general type of interaction between MgO layer and the buffer FeO_{1-x} layer with different point group symmetry. The results show that the reduction of the symmetry of the buffer FeO_{1-x} layer leads to the mixing of different symmetry bands of Fe-bcc bulk electrode, giving them the possibility to interact with MgO oxygen states and therefore to take part in the tunneling process.

Appendix A: LDA+ U approach in MatDCCal code

The main idea of the LDA+ U method is to replace the LDA $e - e$ Coulomb interaction energy of localized electrons in the energy functional of the system by a Hubbard-like term^{14,19,20}:

$$E_{LDA+U}[\rho_\sigma(\mathbf{r}), n_\sigma] = E_{LDA}[\rho_\sigma(\mathbf{r})] + E_U[n_\sigma] - E_{dc}[n_\sigma] \quad (\text{A1})$$

Here $\rho_\sigma(\mathbf{r})$ is a real-space electronic density for spin state σ , $E_{LDA}[\rho_\sigma(\mathbf{r})]$ is a standard LDA functional, and

n_σ is a density matrix of the subsystem of correlated orbitals. The Hubbard-type term of this modified functional can be written in the following way:

$$E_U[n_\sigma] = \frac{1}{2}U \sum_{m,m',\sigma} n_{m\sigma} n_{m'-\sigma} + \frac{1}{2}(U-J) \sum_{m \neq m', m', \sigma} n_{m\sigma} n_{m'\sigma} \quad (\text{A2})$$

Here we assume that the on-site Coulomb (U) and exchange (J) interaction energies are independent of quantum numbers m . This expression also takes into account exchange: the interaction energy is $U - J$ for electrons with the same spin σ , while it is U for electrons with different spin. The last term in (A1) is a so-called ‘‘double counting’’ correction whose role is to subtract from the functional the averaged electron-electron interaction in the correlated subsystem, which has already been taken into account within LDA:

$$E_{dc}[n_\sigma] = \frac{U}{2}N(N-1) - \frac{J}{2} \sum_{\sigma} N_{\sigma}(N_{\sigma}-1) \quad (\text{A3})$$

where N is the total number of electrons in correlated subsystem, and N_{σ} is the total number of electrons with particular spin σ :

$$N_{\sigma} = \sum_m n_{m,\sigma}; \quad N = N_{\sigma} + N_{-\sigma} \quad (\text{A4})$$

Now, by inserting (A2) and (A3) in (A1), and employing the following expression for the total number of particles:

$$N^2 = \sum_{m,\sigma} n_{m\sigma}^2 + \sum_{m \neq m', m', \sigma} n_{m\sigma} n_{m'\sigma} + \sum_{m,m',\sigma} n_{m\sigma} n_{m'-\sigma} \quad (\text{A5})$$

we arrive to a simple and computationally efficient expression for LDA+ U functional:

$$E_{LDA+U} = E_{LDA} + \frac{1}{2}(U-J)(N - \sum_{m,\sigma} n_{m\sigma}^2) \quad (\text{A6})$$

Taking the functional derivative leads to the following expression for the orbital-dependent potential:

$$V_{m\sigma}^{LDA+U} = V_{m\sigma}^{LDA} + \frac{1}{2}(U-J)(1 - 2n_{m\sigma}) \quad (\text{A7})$$

As we notice, this form of LDA+ U potential depends on a single parameter which we call the ‘‘effective’’ Coulomb repulsion $U_{eff} = U - J$. This quantity can be calculated from the first principles for a given atomic system using a constrained LDA approach of Anisimov and Gunnarsson^{14,21}.

To employ this scheme in localized basis set which the MatDcal package uses, we write the orbital-dependent part of the potential in operator form:

$$\hat{V}_{m\sigma} = V_{m\sigma} |m\sigma\rangle \langle m\sigma| \quad (\text{A8})$$

where $V_{m\sigma}$ is the second term in (A7), and $|m\sigma\rangle \langle m\sigma|$ is a projection operator on the atomic orbital basis function corresponding to the localized state, for which LDA+ U treatment is applied. In this form we add the LDA+ U potential in a straightforward manner to the MatD-CAL software where the Hamiltonian matrix elements are calculated. Having computed the matrix elements, we follow the standard computational scheme of NEGF method in localized basis set representation. The technical details of this implementation can be found in several previous publications^{13,16,23}.

* Electronic address: vladimir@physics.mcgill.ca

¹ S. Yuasa, T. Nagahama, A. Fukushima, Y. Suzuki, and K. Ando, Nat. Mater. **3**, 868 (2004).
² S. Parkin, C. Kaiser, A. Panchula, P. Rice, B. Hughes, M. Samant, and S.-H. Yang, Nat. Mater. **3**, 862 (2004).
³ J. Moodera, L. Kinder, T. Wong, and R. Meservey, Phys. Rev. Lett. **74**, 3273 (1995).
⁴ A. Ney, C. Pampuch, R. Koch, and K. Ploog, Nature (London) **425**, 485 (2003).
⁵ W. Butler, X.-G. Zhang, and T. Schulthess, Phys. Rev. B **63**, 054416 (2001).
⁶ D. Waldron, V. Timoshevskii, Y. Hu, K. Xia, and H. Guo, Phys. Rev. Lett. **97**, 226802 (2006).
⁷ J. C. R. P. G. Mather and R. A. Buhrman, Phys. Rev. B **73**, 205412 (2006).
⁸ K. X. Y. Q. Ke and H. Guo, Phys. Rev. Lett. **105**, 236801 (2010).

⁹ H. M. et al., Phys. Rev. Lett. **87**, 076102 (2001).
¹⁰ X.-G. Zhang, W. Butler, and A. Bandyopadhyay, Phys. Rev. B **68**, 092402 (2003).
¹¹ G. M. et al., Phys. Rev. Lett. **100**, 246803 (2008).
¹² S. Mirhosseini, K. Saha, A. Ernst, and J. Henk, Phys. Rev. B **78**, 012404 (2008).
¹³ J. Taylor, H. Guo, and J. Wang, Phys. Rev. B **63**, 121104 (2001).
¹⁴ V. Anisimov and O. Gunnarsson, Phys. Rev. B **43**, 7570 (1991).
¹⁵ P. Blaha, K. Schwarz, G. Madsen, D. Kvasnicka and J. Luitz, WIEN2k, An Augmented Plane Wave + Local Orbitals Program for Calculating Crystal Properties (Karlheinz Schwarz, Techn. Universitt Wien, Austria), 2001. ISBN 3-9501031-1-2.
¹⁶ Matdcal reference ...
¹⁷ N. Troullier and J.L. Martins, Phys. Rev. B **43**, 1993

- (1991); K. Kleinman and D.M. Bylander, Phys. Rev. Lett. **48**, 1425 (1982).
- ¹⁸ D. Waldron, P. Haney, B. Larade, A. MacDonald, and H. Guo, Phys. Rev. Lett. **96**, 166804 (2006).
- ¹⁹ V. Anisimov, J. Zaanen, and O. Andersen, Phys. Rev. B **44**, 943 (1991).
- ²⁰ V. Anisimov, I. Solovyev, M. Korotin, M. Czyżyk, and G. Sawatzky, Phys. Rev. B **48**, 16929 (1993).
- ²¹ G. Madsen and P. Novák, Europhys. Lett. **69**, 777 (2005).
- ²² Due to the semiinfinite nature of the iron lead, we assume the geometry of the electronic wavefunction, entering the FeO_{0.5} layer, to be the same as in the lead (Fe-bcc cubic lattice). However, the square lattice of FeO_{0.5} layer, as well as the MgO lattice, are 45° rotated with respect to Fe-bcc unit cell. This fact is taken into consideration when we classify Fe states, coming out of the lead, in the new symmetry of FeO_{0.5} and MgO layers. The most important in this context is that the $d_{x^2-y^2}$ orbital, which significant contribution to the scattering states was obtained by numerical computations, is in fact the d_{xy} orbital in Fe-bcc lattice.
- ²³ E. Marcotte, M.Sc. thesis, McGill University. (2009).